RSC Advances

PAPER

View Article Online
View Journal | View Issue

Cite this: *RSC Adv.*, 2022, **12**, 1638

A thiadiazolopyridine-functionalized Zr(IV)-based metal–organic framework for enhanced photocatalytic synthesis of tetrahydroquinolines under visible light†

Changyun Li,‡[a] He Zhang,‡[a] Xuefei Wang,[a] Qiu-Yan Li,*[a] Xinsheng Zhao[b] and Xiao-Jun Wang*[a]

Metal–organic framework (MOF) materials provide a versatile and promising platform for constructing heterogeneous photocatalysts with applications in organic transformations. One of the methods for enhancing MOFs' performance in photocatalysis relies on the elaborate design and functionalization of organic linkers. Here we reported a photoactive thiadiazolopyridine (TDP) moiety functionalized UiO-68 isoreticular Zr(IV)-based MOF (denoted as UiO-68-TDP) that was synthesized by the *de novo* approach of mixed dicarboxylate struts. Under blue LED irradiation and in an open air atmosphere, MOF UiO-68-TDP exhibited a largely higher photocatalytic activity for the synthesis of tetrahydroquinolines by oxidative annulation reaction between *N*,*N*-dimethylanilines and maleimides, in comparison to the benzothiadiazole decorated analogue MOF. Besides, UiO-68-TDP can be reused at least three times without significant loss of its photocatalytic activity and its framework was well maintained after these cycles. Furthermore, the related mechanism involving reactive oxygen species was properly proposed.

Received 3rd October 2021
Accepted 13th December 2021

DOI: 10.1039/d1ra07363j

rsc.li/rsc-advances

Introduction

Visible light is regarded as an abundant, inexpensive, readily available and renewable source of clean energy. Its application in synthesis of value-added organic compounds has received great attention from chemists over the past years.[1–5] However, since a large proportion of simple organic molecules cannot absorb visible light, photocatalysts such as metal complexes and organic dyes are typically used to efficiently promote the photochemical transformation.[6–9]

The tetrahydroquinoline (THQ) motif is an important structural scaffold of many natural products and medicinal agents that have demonstrated a variety of biological activities.[10,11] Due to their widespread existence in natural products and pharmaceutical agents, a number of methods have been developed for the construction of THQ skeleton.[12–14] Among them, the photochemical approach mediated by visible light offered a more sustainable methodology in this process.[15–18] However, most of these photochemical reactions were conducted in homogenous systems. Thus, it is problematic to recycle these photocatalysts for reuse, especially considering the high cost of precious metal complexes. The development of heterogeneous photocatalysts that are free of noble metals as well as possessing outstanding catalytic activity is highly desirable. In this regard, there are only a handful of reported examples to date.[19–21] For example, Zhang *et al.* developed a series of benzobisthiadiazole conjugated nanoporous polymers for the synthesis of THQ derivatives under visible light.[19] Modified TiO_2 semiconductors were also employed as efficient photocatalysts in this photochemical reaction.[20,21] However, the reported heterogeneous photocatalyst based materials are still limited and suffered from some drawbacks, such as tedious preparative procedure and low surface area. It is highly demanded to exploit more different materials toward this end.

Metal–organic frameworks (MOFs), that are assembled by the coordination of metal centers with organic linkers, have emerged as a newly promising type of photoactive materials for photocatalyzing organic reactions on account of their unique structural characteristics.[22–25] In sharp contrast to metal oxide semiconductive photocatalysts, the hybrid and modular inherent nature of MOF materials allows their properties to be readily tailored by the metal nodes, organic linkers as well as the cavity in MOFs, thus resulting in the remarkable enhancement of photocatalytic activities. Our research group has recently devoted many efforts into the modulation of MOFs photocatalytic performance starting from the design and

[a]*Jiangsu Key Laboratory of Green Synthetic Chemistry for Functional Materials, School of Chemistry and Materials Science, Jiangsu Normal University, Xuzhou 221116, P. R. China*

[b]*School of Physics and Electronic Engineering, Jiangsu Normal University, Xuzhou 221116, P. R. China. E-mail: qyli@jsnu.edu.cn; xjwang@jsnu.edu.cn*

† Electronic supplementary information (ESI) available. See DOI: 10.1039/d1ra07363j

‡ These authors have contributed equally to this work.

synthesis of photoactive organic linkers; subsequently, a series of functional and robust Zr(IV) MOFs with UiO-isoreticular topology were constructed by using these linkers and their applications in light-induced organic reactions were further explored.[26–30] To the best of our knowledge, there is no report that MOFs photocatalyzed THQ synthesis until now.

Along our research line in functionalization of organic linkers, here we designed and synthesized a photoactive thiadiazolopyridine (TDP) moiety[31–33] conjugated terphenyldicarboxylate linker (denoted as H_2-TDP), which was integrated into the porous and robust UiO-68 isoreticular Zr-MOF (denoted as UiO-68-TDP, Scheme 1) by a mix-and-match approach of mixed dicarboxylate struts. In the open air atmosphere and under blue LEDs irradiation, UiO-68-TDP can efficiently photocatalyze the oxidative cyclization synthesis of THQs from *N*,*N*-dimethylanilines and maleimides. And it demonstrated a remarkably higher photocatalytic activity for this reaction than its analogue MOF UiO-68-BTD containing the benzothiadiazole (BTD) unit.

Results and discussion

As described in Scheme 2, the TDP-conjugated terphenyldicarboxylate linker (H_2-TDP) can be readily synthesized by two step reactions. The well-known Suzuki coupling reaction of 4,7-dibromo-[1,2,5]thiadiazolo[3,4-*c*]pyridine (**1**) and methyl 4-boronobenzoate catalyzed by $Pd(dppf)Cl_2$ and $Pd(PPh_3)_4$ in the presence of Cs_2CO_3 and CsF gave rise to methyl ester precursor compound **2**, which further hydrolyzed by KOH to give the target linker H_2-TDP in a high yield. Due to limited solubility of H_2-TDP, the mix-and-match synthetic strategy was used to incorporate it into the porous and robust UiO-68 framework. Specifically, a combination of organic linkers H_2-TDP and H_2-DMT (in 1 : 3 molar ratio) with the same ligand length was reacted with $ZrCl_4$ under the assistance of HAc as a modulator in *N*,*N*-dimethylformamide (DMF) at 90 °C for 48 h to generate MOF UiO-68-TDP (Scheme 1).

As expected, powder X-ray diffraction (XRD) of UiO-68-TDP was investigated to reveal its isostructural framework as the same with the parent MOF UiO-68 and its highly crystalline

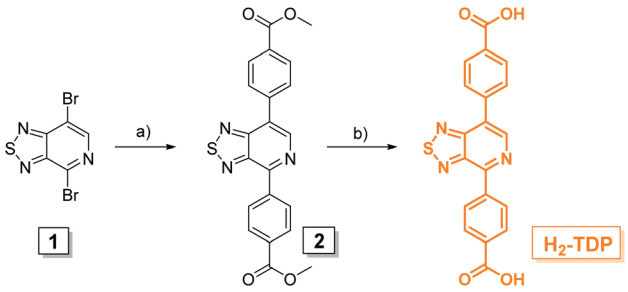

Scheme 2 Synthetic route for H_2-TDP. Reagents and conditions: (a) Cs_2CO_3, CsF, $Pd(PPh_3)_4$, $Pd(dppf)Cl_2$, toluene–H_2O, 90 °C for 2 d; (b) KOH, THF, CH_3OH, H_2O, 90 °C for 2 h; TFA, H_2O, 0.5 h, room temperature.

nature (Fig. 1a). Additionally, the porosity of UiO-68-TDP was examined by nitrogen sorption measurement at 77 K (Fig. 1b), indicating a classic type I reversible isotherm with BET surface area of 3060 $m^2\ g^{-1}$. The pore size distribution was calculated as ~1.6 nm by using nonlocal density functional theory (NLDFT). Therefore, the high porosity and big pore width of UiO-68-TDP can facilitate adsorption and diffusion of substrates in the framework for achieving an efficient heterogeneous catalysis.

In order to evaluate the photocatalytic activity of UiO-68-TDP, the oxidative annulation reaction of *N*,*N*-dimethylaniline (**1a**, 0.2 mmol) and *N*-(4-methylphenyl)maleimide (**2a**, 0.1 mmol) was employed as a model reaction. As shown in Table 1, the reaction mixture of **1a** and **2a** containing a catalytic amount of UiO-68-TDP in CH_3CN was irradiated by blue LEDs in an open air atmosphere at room temperature. The desired annulation product of THQ derivative **3a** can be optimized and obtained in good-to-excellent yield after 12 h irradiation (entries 1–3). The very low yield was achieved in the absence of UiO-68-TDP (entry 4), confirming its photocatalytically active role in this reaction. On the other hand, when the photocatalyst was changed from UiO-68-TDP into its analogue MOF UiO-68-BTD containing benzothiadiazole moiety (Fig. S4 in ESI†), the product yield of **3a** was largely decreased (entry 5). Furthermore, we monitored and compared this photocatalytic progress by using ^1H NMR analysis. As shown in Fig. 2a, it is clear that UiO-

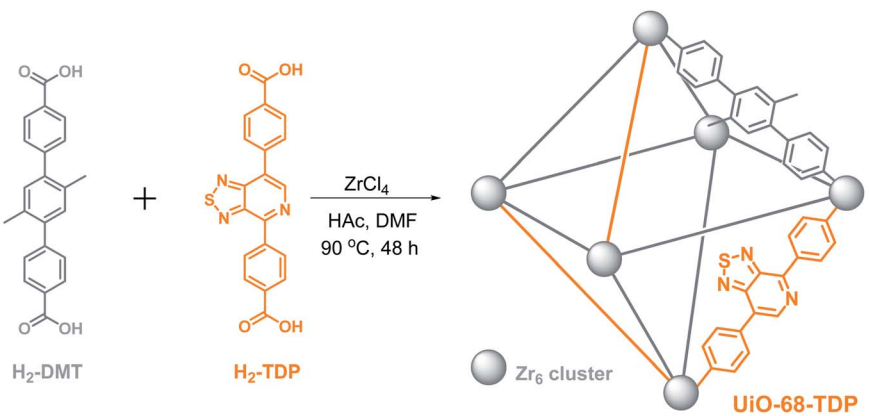

Scheme 1 Preparation for MOF UiO-68-TDP with the mixed dicarboxylate linkers.

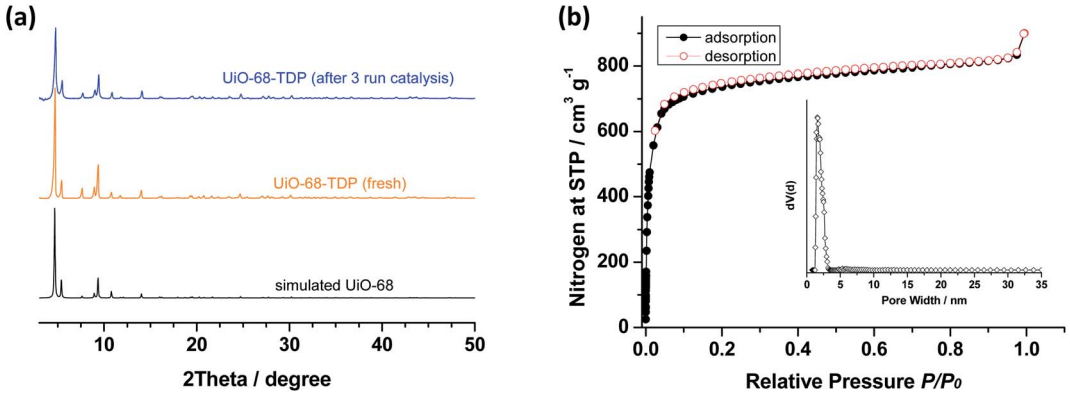

Fig. 1 Powder XRD patterns (a) and nitrogen sorption isotherm (b) for UiO-68-TDP (inset: the pore size distribution calculated from NLDFT).

Table 1 Screening of the photocatalytic reaction conditions of **1a** and **2a**[a]

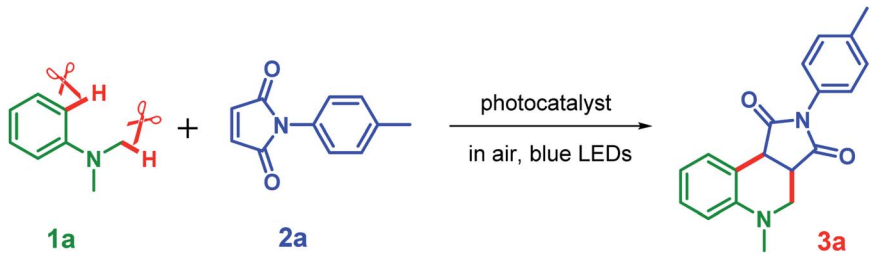

Entry	Conditions	Light	Additive	Yield[b]
1	UiO-68-TDP, 3 mg	+	—	62%
2	UiO-68-TDP, 4 mg	+	—	82%
3	UiO-68-TDP, 5 mg	+	—	82%
4	No photocatalyst	+	—	12%
5[c]	UiO-68-BTD, 4 mg	+	—	16%
6[d]	UiO-68-TDP, 4 mg	—	—	Trace
7[e]	UiO-68-TDP, 4 mg	+	—	Trace
8[f]	UiO-68-TDP, 4 mg	+	BQ	8%
9[g]	UiO-68-TDP, 4 mg	+	NaN_3	16%

[a] Reaction conditions: **1a** (0.2 mmol), **2a** (0.1 mmol) in CH_3CN (1 mL) under an air atmosphere at room temperature for 12 h, blue LEDs (λ_{max} = 450 nm, 3 W). [b] Yield was determined by ^1H NMR analysis with 1-methyl-2,4-dinitrobenzene as an internal standard. [c] The reaction time was 16 h. [d] No light. [e] No oxygen. [f] *p*-Benzoquinone (BQ) as the superoxide scavenger. [g] NaN_3 as the single oxygen $^1O_2$ scavenger.

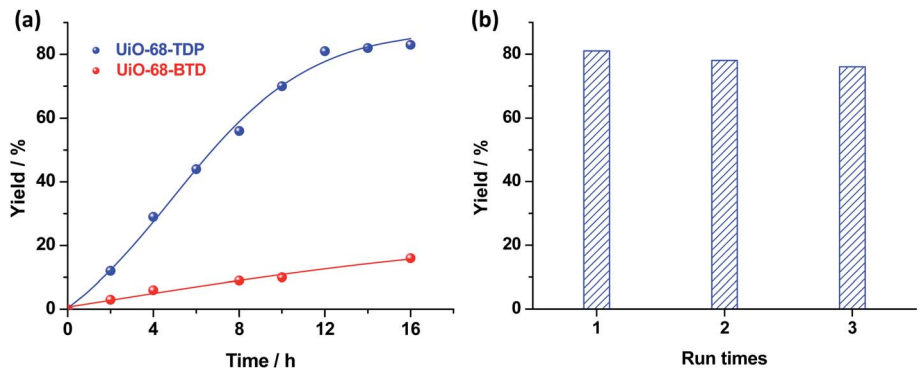

Fig. 2 (a) Photocatalytic profiles of oxidative annulation reaction between *N*,*N*-dimethylaniline (**1a**) and *N*-(4-methylphenyl)maleimide (**2a**) by UiO-68-TDP and UiO-68-BTD under the irradiation of blue-LEDs in an open air atmosphere. (b) Recycling experiments of UiO-68-TDP for the photocatalyzed oxidative annulation reaction.

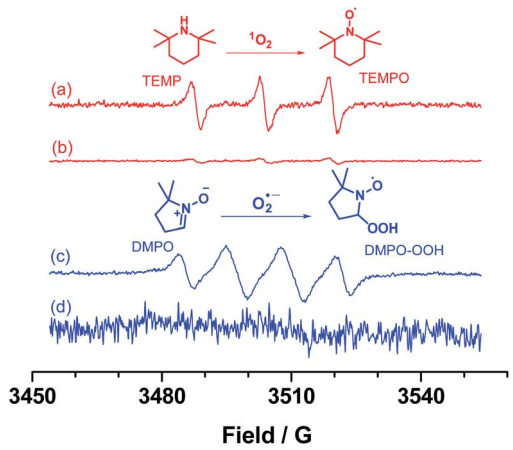

Fig. 3 EPR spectra of a mixture of UiO-68-TDP in CH_3CN with TEMP upon light irradiation (a) and in the dark (b) as well as DMPO upon light irradiation (c) and in the dark (d).

68-TDP exhibited a largely higher photocatalytic activity for this light-induced oxidative annulation reaction in contrast to UiO-68-BTD. This result validates the critical role of photoactive organic linker in determining MOF's photocatalytic performance. Besides, the reusability of UiO-68-TDP as a heterogeneous photocatalyst was investigated. The MOF photocatalyst can be readily recovered from the reaction mixture by centrifugation and reused at least three times without obvious loss of activity (Fig. 2b). The powder XRD pattern of UiO-68-TDP after three photocatalyzed cycles revealed the good maintenance of its crystalline structure and framework (Fig. 1a), indicative of the high stability of Zr-based UiO frameworks.

To gain insights into the photochemical reaction mechanism, several control experiments were conducted as shown in Table 1 (entries 6–9). These results indicated that each component, including photocatalyst UiO-68-TDP, light, and oxygen, is essential for the effective progress in the photo-induced reaction. Additionally, *p*-benzoquinone (BQ) and NaN_3, as a superoxide radical anion $O_2^{\bullet-}$ scavenger and a singlet oxygen $^1O_2$ scavenger, were added into the reaction mixture, respectively. The product yield was greatly decreased (entries 8 and 9), suggesting that both of active oxygen species ($O_2^{\bullet-}$and $^1O_2$) were involved in this photo-oxidative annulation reaction. Furthermore, electron paramagnetic resonance (EPR) measurements were employed to validate these oxygen active species by using DMPO and TEMP as spin-trapping reagents for $O_2^{\bullet-}$and $^1O_2$ after blue LEDs light irradiation. As shown in Fig. 3, no signal was observed for the mixture of UiO-68-TDP with TEMP or DMPO in the dark condition. While the typically characteristic of $^1O_2$ and $O_2^{\bullet-}$ corresponding TEMPO and DMPO–OOH were clearly detected in EPR spectra (Fig. 3a and c), these results suggest the effective energy transfer and/or electron transfer between excited UiO-68-TDP species to molecular oxygen during the photocatalytic process.

Based on these observations in the above control experiments and reported literatures, we proposed a plausible reaction mechanism for the formation of THQ derivative **3a**, as

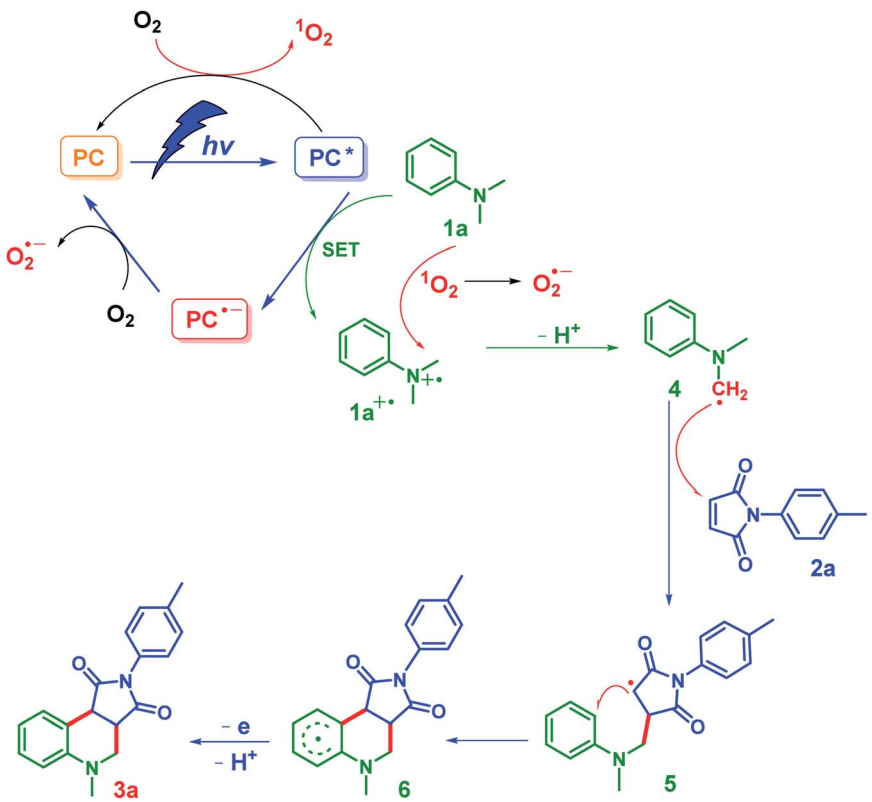

Scheme 3 Proposed mechanism for the photocatalytic oxidative annulation reaction by MOF UiO-68-TDP (photocatalyst, PC).

Table 2 Photocatalytic oxidative cyclization of various *N*,*N*-dimethylanilines with maleimides by MOF UiO-68-TDP[a]

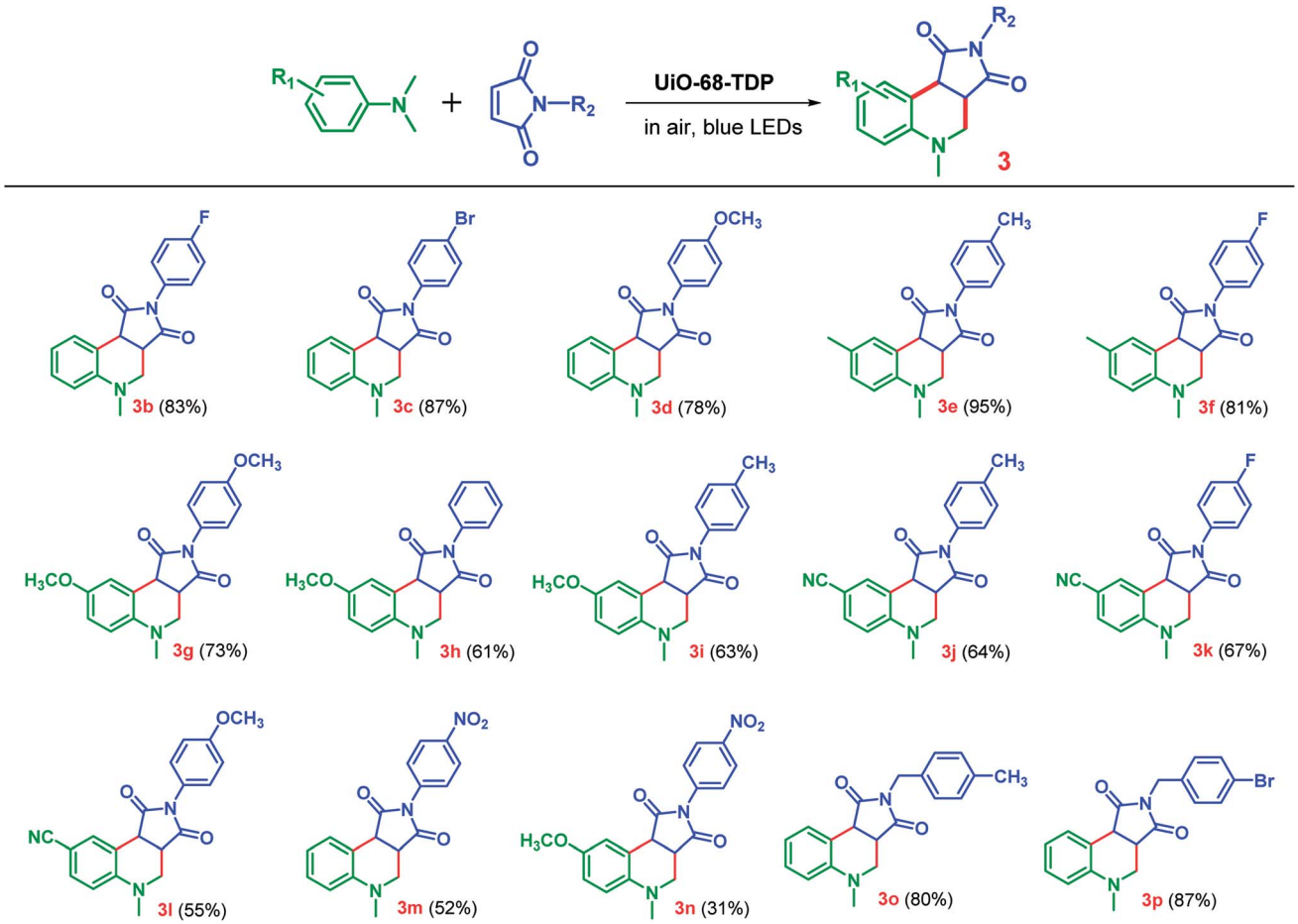

[a] Reaction conditions: *N*,*N*-dimethylanilines (0.2 mmol), maleimides (0.1 mmol) and MOF UiO-68-TDP (4 mg) in CH_3CN (1 mL) under an air atmosphere at room temperature for 12 h, blue LEDs (λ_{max} = 450 nm, 3 W). Yield was determined by ^{1}H-NMR analysis with 1-methyl-2,4-dinitrobenzene as an internal standard.

illustrated in Scheme 3. Upon light illumination, MOF UiO-68-TDP as photocatalyst (PC) was excited from the ground state to its excited state (PC*), which can activate molecular oxygen O_2 through energy transfer or single electron transfer (SET) process, generating two reactive oxygen species of $^1O_2$ and $O_2^{\cdot-}$. Simultaneously, the radical cation **1a**$^{\cdot+}$ was produced in the oxidation of **1a** by PC* and $^1O_2$ through a SET process, which was deprotonated by the superoxide anion radical to give α-aminoalkyl radical **4**. Then, the radical addition of **4** to maleimide **2a** formed radical **5**, along with the subsequent intramolecular cyclization leading to intermediate **6**. At last, the electron and proton separation from **6** mediated by active oxygen species gave birth to the desired product **3a**.

Furthermore, the scope of this photocatalytic reaction was investigated to explore its broad applications by varying substrates with both electron-donating and electron-withdrawing groups under the same reaction conditions using UiO-68-TDP as photocatalyst. As shown in Table 2, most of reactions can afford modest to good yields. A range of *N*,*N*-dimethylanilines with methyl, methoxy and cyano groups on the phenyl ring can react with various maleimides to afford the corresponding THQ derivatives in good to excellent yields (**3b–3l**, 55–95%), while maleimides with a nitro group gave a relative poor yield (**3m–3n**, 31–52%). Besides, a very good yield can be obtained by using benzyl substituted maleimides (**3o–3p**, 80–87%).

Conclusions

In summary, we have conjugated a photoactive thiadiazolopyridine moiety into the terphenyldicarboxylate linker, which was subsequently integrated into the porous and robust UiO-type isoreticular Zr-MOF UiO-68-TDP by a mix-and-match approach using mixed dicarboxylate struts. In the open air atmosphere, UiO-68-TDP can efficiently photocatalyze the oxidative cyclization synthesis of tetrahydroquinolines from *N*,*N*-dimethylanilines and maleimides under blue-LED irradiation. Moderate to high yields were achieved from a wide

range of substrates by using UiO-68-TDP as heterogeneous photocatalyst under this reaction conditions. In comparison to its analogue UiO-68-BTD containing benzothiadiazole unit, UiO-68-TDP demonstrated a remarkably higher photocatalytic activity for this reaction. This work demonstrates the great potential of MOF based photocatalysts as well as the critical role of organic linker design in determining MOF's photocatalytic performance.

Experimental section

Synthesis and characterizations

Compound 2. A mixture of Cs_2CO_3 (12.3 g, 37.6 mmol) and CsF (0.95 g, 6.25 mmol) were dissolved in water (2 mL) and added into a 250 mL round bottom flask with a magnetic stir bar. Toluene (140 mL) was added into the reaction flask and the reaction mixture was bubbling by N_2 for 3 h. Then, compound **1** (1.85 g, 6.3 mmol), methyl 4-boronobenzoate (3.4 g, 18.8 mmol), $Pd(dppf)Cl_2$ (0.54 g, 0.62 mmol) and $Pd(PPh_3)_4$ (0.72 g, 0.62 mmol) were added into the mixture. The round bottom flask was vacuumed and purged into N_2 for 4 times. The reaction was heated at 90 °C for 48 hours under nitrogen atmosphere. After that, the reaction mixture was cooled down to room temperature and extracted by CH_2Cl_2 (200 mL × 2). The combined organic layer was washed with water (300 mL × 5), and dried over anhydrous Na_2SO_4 then evaporated under reduced pressure. The crude product was further purified using column chromatograph (CH_2Cl_2/PE, 6/1) to give orange solid (2.03 g, yield: 80%). ^{1}H NMR (400 MHz, $CDCl_3$) δ 8.92 (s, 1H), 8.75 (d, J = 8.5 Hz, 2H), 8.25 (dd, J = 8.4, 4.1 Hz, 4H), 8.12 (d, J = 8.4 Hz, 2H), 3.99 (s, 6H).

Compound H_2-TDP. Compound **2** (0.50 g, 1.23 mmol) was dissolved in THF (10 mL) and added into a 100 mL round bottom flask with a magnetic stir bar. KOH (1.03 g, 19.58 mmol) was dissolved in MeOH (5 mL) and added into the mixture which was refluxed for 0.5 h at 90 °C. Then, 5 mL water was added into the above reaction, which was subsequently stirred at 90 °C for 1.5 h. After cooling to room temperature, 3 mL TFA was added and stirred for 30 min. Then, 20 mL water was further added into the mixture. The solid was obtained by centrifugal to get the crude product, and washed for 3 times by water and dried to give yellow powder solid (0.40 g, yield: 86%). ^{1}H NMR (400 MHz, DMSO-d_6) δ 13.02 (s, 2H), 9.07 (s, 1H), 8.75 (d, J = 8.3 Hz, 2H), 8.26 (d, J = 8.2 Hz, 2H), 8.18 (dd, J = 14.2, 8.3 Hz, 4H).

MOF UiO-68-TDP. H_2-DMT (69 mg, 0.20 mmol), H_2-TDP (25 mg, 0.067 mmol) and $ZrCl_4$ (74 mg, 0.32 mmol) were dissolved in DMF (100 mL), which was added into a 250 mL round bottom flask with a magnetic stir bar. Then, HAc (4 mL) was added to the reaction flask and the reaction mixture was heated at 90 °C for 48 hours. After cooling to room temperature, the product was separated by centrifugal to afford the golden solid which was washed with DMF (10 mL × 3) and EtOH (10 mL × 3), respectively. The sample was dried in vacuum. The powder XRD pattern of product was similar to the simulated pattern, confirming its UiO-68 topological framework and the phase purity.

Conflicts of interest

There are no conflicts to declare.

Acknowledgements

The work was financially supported from Natural Science Foundation of Jiangsu Province (BK20181001).

References

1 D. M. Schultz and T. P. Yoon, Solar Synthesis: Prospects in Visible Light Photocatalysis, *Science*, 2014, **343**, 1239176.
2 N. A. Romero and D. A. Nicewicz, Organic Photoredox Catalysis, *Chem. Rev.*, 2016, **116**, 10075–10166.
3 J. Xie, H. Jin and A. S. K. Hashmi, The Recent Achievements of Redox-Neutral Radical C-C Cross-Coupling Enabled by Visible-Light, *Chem. Soc. Rev.*, 2017, **46**, 5193–5203.
4 B. Chen, L.-Z. Wu and C.-H. Tung, Photocatalytic Activation of Less Reactive Bonds and Their Functionalization Via Hydrogen-Evolution Cross-Couplings, *Acc. Chem. Res.*, 2018, **51**, 2512–2523.
5 X.-Y. Yu, J.-R. Chen and W.-J. Xiao, Visible Light-Driven Radical-Mediated C–C Bond Cleavage/Functionalization in Organic Synthesis, *Chem. Rev.*, 2021, **121**, 506–561.
6 C. K. Prier, D. A. Rankic and D. W. C. MacMillan, Visible Light Photoredox Catalysis with Transition Metal Complexes: Applications in Organic Synthesis, *Chem. Rev.*, 2013, **113**, 5322–5363.
7 X. Huang and E. Meggers, Asymmetric Photocatalysis with Bis-Cyclometalated Rhodium Complexes, *Acc. Chem. Res.*, 2019, **52**, 833–847.
8 A. Tlili and S. Lakhdar, Acridinium Salts and Cyanoarenes as Powerful Photocatalysts: Opportunities in Organic Synthesis, *Angew. Chem., Int. Ed.*, 2021, **60**, 19526–19549.
9 J. D. Bell and J. A. Murphy, Recent Advances in Visible Light-Activated Radical Coupling Reactions Triggered by (i) Ruthenium, (ii) Iridium and (Iii) Organic Photoredox Agents, *Chem. Soc. Rev.*, 2021, **50**, 9540–9685.
10 N. Goli, P. S. Mainkar, S. S. Kotapalli, T. K, R. Ummanni and S. Chandrasekhar, Expanding the Tetrahydroquinoline Pharmacophore, *Bioorg. Med. Chem. Lett.*, 2017, **27**, 1714–1720.
11 J. Liu, G. S. Cremosnik, F. Otte, A. Pahl, S. Sievers, C. Strohmann and H. Waldmann, Design, Synthesis, and Biological Evaluation of Chemically and Biologically Diverse Pyrroquinoline Pseudo Natural Products, *Angew. Chem., Int. Ed.*, 2021, **60**, 4648–4656.
12 V. Sridharan, P. A. Suryavanshi and J. C. Menéndez, Advances in the Chemistry of Tetrahydroquinolines, *Chem. Rev.*, 2011, **111**, 7157–7259.
13 I. Muthukrishnan, V. Sridharan and J. Carlos Menendez, Progress in the Chemistry of Tetrahydroquinolines, *Chem. Rev.*, 2019, **119**, 5057–5191.
14 N. Hofmann, L. Homberg and K. C. Hultzsch, Synthesis of Tetrahydroquinolines Via Borrowing Hydrogen

Methodology Using a Manganese Pn3 Pincer Catalyst, *Org. Lett.*, 2020, **22**, 7964–7970.

15 T. P. Nicholls, G. E. Constable, J. C. Robertson, M. G. Gardiner and A. C. Bissember, Bronsted Acid Cocatalysis in Copper(I)-Photocatalyzed Alpha-Amino C–H Bond Functionalization, *ACS Catal.*, 2016, **6**, 451–457.

16 J.-T. Guo, D.-C. Yang, Z. Guan and Y.-H. He, Chlorophyll-Catalyzed Visible-Light-Mediated Synthesis of Tetrahydroquinolines from *N*,*N*-Dimethylanilines and Maleimides, *J. Org. Chem.*, 2017, **82**, 1888–1894.

17 X.-L. Yang, J.-D. Guo, T. Lei, B. Chen, C.-H. Tung and L.-Z. Wu, Oxidative Cyclization Synthesis of Tetrahydroquinolines and Reductive Hydrogenation of Maleimides under Redox-Neutral Conditions, *Org. Lett.*, 2018, **20**, 2916–2920.

18 C.-W. Hsu and H. Sunden, Alpha-Aminoalkyl Radical Addition to Maleimides Via Electron Donor-Acceptor Complexes, *Org. Lett.*, 2018, **20**, 2051–2054.

19 Z. J. Wang, S. Ghasimi, K. Landfester and K. A. I. Zhang, Bandgap Engineering of Conjugated Nanoporous Poly-Benzobisthiadiazoles Via Copolymerization for Enhanced Photocatalytic 1,2,3,4-Tetrahydroquinoline Synthesis under Visible Light, *Adv. Synth. Catal.*, 2016, **358**, 2576–2582.

20 J. Tang, G. Grampp, Y. Liu, B.-X. Wang, F.-F. Tao, L.-J. Wang, X.-Z. Liang, H.-Q. Xiao and Y.-M. Shen, Visible Light Mediated Cyclization of Tertiary Anilines with Maleimides Using Nickel(Ii) Oxide Surface-Modified Titanium Dioxide Catalyst, *J. Org. Chem.*, 2015, **80**, 2724–2732.

21 M. Hosseini-Sarvari, M. Koohgard, S. Firoozi, A. Mohajeri and H. Tavakolian, Alizarin Red S–TiO_2-Catalyzed Cascade C(sp^3)–H to C(sp^2)–H Bond Formation/Cyclization Reactions toward Tetrahydroquinoline Derivatives under Visible Light Irradiation, *New J. Chem.*, 2018, **42**, 6880–6888.

22 T. Zhang and W. Lin, Metal–Organic Frameworks for Artificial Photosynthesis and Photocatalysis, *Chem. Soc. Rev.*, 2014, **43**, 5982–5993.

23 X. Deng, Z. Li and H. Garcia, Visible Light Induced Organic Transformations Using Metal–Organic-Frameworks (Mofs), *Chem.–Eur. J.*, 2017, **23**, 11189–11209.

24 Y. Fang, Y. Ma, M. Zheng, P. Yang, A. M. Asiri and X. Wang, Metal–Organic Frameworks for Solar Energy Conversion by Photoredox Catalysis, *Coord. Chem. Rev.*, 2018, **373**, 83–115.

25 T. Zhang, Y. Jin, Y. Shi, M. Li, J. Li and C. Duan, Modulating Photoelectronic Performance of Metal–Organic Frameworks for Premium Photocatalysis, *Coord. Chem. Rev.*, 2019, **380**, 201–229.

26 Q.-Y. Li, Z. Ma, W.-Q. Zhang, J.-L. Xu, W. Wei, H. Lu, X. Zhao and X.-J. Wang, Aie-Active Tetraphenylethene Functionalized Metal–Organic Framework for Selective Detection of Nitroaromatic Explosives and Organic Photocatalysis, *Chem. Commun.*, 2016, **52**, 11284–11287.

27 W.-Q. Zhang, Q.-Y. Li, Q. Zhang, Y. Lu, H. Lu, W. Wang, X. Zhao and X.-J. Wang, Robust Metal–Organic Framework Containing Benzoselenadiazole for Highly Efficient Aerobic Cross-Dehydrogenative Coupling Reactions under Visible Light, *Inorg. Chem.*, 2016, **55**, 1005–1007.

28 W.-Q. Zhang, Q.-Y. Li, X. Yang, Z. Ma, H. Wang and X.-J. Wang, Benzothiadiazole Conjugated Metal–Organic Framework for Organic Aerobic Oxidation Reactions under Visible Light, *Acta Chim. Sinica*, 2017, **75**, 80–85.

29 W.-Q. Zhang, Q.-Y. Li, J.-Y. Cheng, K. Cheng, X. Yang, Y. Li, X. Zhao and X.-J. Wang, Ratiometric Luminescent Detection of Organic Amines Due to the Induced Lactam–Lactim Tautomerization of Organic Linker in a Metal–Organic Framework, *ACS Appl. Mater. Interfaces*, 2017, **9**, 31352–31356.

30 W.-Q. Zhang, K. Cheng, H. Zhang, Q.-Y. Li, Z. Ma, Z. Wang, J. Sheng, Y. Li, X. Zhao and X.-J. Wang, Highly Efficient and Selective Photooxidation of Sulfur Mustard Simulant by a Triazolobenzothiadiazole-Moiety-Functionalized Metal–Organic Framework in Air, *Inorg. Chem.*, 2018, **57**, 4230–4233.

31 Y. Ji, B. He, H. Lu, J. Xu, R. Wang, Y. Jin, C. Zhong, Y. Shan, F. Wu and L. Zhu, Core Structure Engineering in Hole-Transport Materials to Achieve Highly Efficient Perovskite Solar Cells, *Chemsuschem*, 2019, **12**, 1374–1380.

32 B. Wang, M. Wang, A. Mikhailovsky, S. Wang and G. C. Bazan, A Membrane-Intercalating Conjugated Oligoelectrolyte with High-Efficiency Photodynamic Antimicrobial Activity, *Angew. Chem., Int. Ed.*, 2017, **56**, 5031–5034.

33 T. Ishi-i, H. Tanaka, H. Koga, Y. Tanaka and T. Matsumoto, Near-Infrared Fluorescent Organic Porous Crystal That Responds to Solvent Vapors, *J. Mater. Chem. C*, 2020, **8**, 12437–12444.